Hindawi
Mathematical Problems in Engineering
Volume 2019, Article ID 1748679, 9 pages
https://doi.org/10.1155/2019/1748679

Research Article

Dynamic Analysis of a Novel Rail-Grinding Car Using Open-Structured Abrasive Belt for High-Speed Railways

Wengang Fan,[1,2] Guangyou Hou,[1,2] Wenxi Wang ,[1,2] and Yuefeng Wu[3]

[1]*School of Mechanical, Electronic, and Control Engineering, Beijing Jiaotong University, Beijing 100044, China*
[2]*Key Laboratory of Vehicle Advanced Manufacturing, Measuring and Control Technology, Ministry of Education, Beijing 100044, China*
[3]*Shijiazhuang Railway Station, China Railway Beijing Group Co., Ltd., Shijiazhuang 050051, China*

Correspondence should be addressed to Wenxi Wang; 14116345@bjtu.edu.cn

Received 20 February 2019; Revised 19 April 2019; Accepted 7 May 2019; Published 22 May 2019

Academic Editor: Roberto G. Citarella

Nowadays, applying rail grinding has been worldwide recognized as the routine maintenance approach to improving the wheel-rail relationship, as well as extending the rail's serving life. However, the traditional rail repair technology with the abrasive wheel or the milling cutter is getting harder to meet the increasing demand for high efficiency with high speed. In this paper, according to the engineering requirements and constraints, a new fast rail-grinding car based on open-structured belt grinding technology was designed for the corrugation treatment on high-speed railways. A corresponding simulation model was established and its dynamic working performance was then assessed by SIMPACK software. Results of the four dynamic indices for both straight and curve tracks were within the limits, which had verified the design rationality of the new rail-grinding car. Those dynamic indices are the lateral vibration acceleration, the vertical vibration acceleration, the axle transverse force, and the derailment coefficient.

1. Introduction

The rail has been the key component of the railway transport system in the world for more than a century. Due to the harsh service environment induced by the complex vehicle-track interaction, its surface and interior are vulnerable to kinds of defects, including crack and corrugation [1, 2]. Those defects can eventually lead to the partial or complete failure of the rail and even cause the derailment accident. Thus, rail grinding has been widely adopted by most countries to improve the wheel-rail matching relationship, to prolong the rail's serving life, and also to strengthen the train's running stability [3, 4].

To date, several kinds of rail-grinding technologies have been applied in the practical engineering, such as the facing grinding by abrasive wheel [5–8], the peripheral grinding by abrasive wheel [9, 10], and the milling by combined cutter blades [11]. Each technology has its own limitation and application field due to its characteristics. For example, the milling by combined cutter blades is restricted only for the corrective maintenance of the severely worn or defective rails. Recently, based on theoretical analysis and test, the rail-grinding process using abrasive belt [12, 13] has shown some specific advantages in metal removal rate, surface quality and dust collection, etc. It seems to be potentially one of the most recognized technologies for rail maintenance in the near future.

Incontrovertibly, the growing running speed and the diminishing maintenance time are becoming a huge challenge to the rail-grinding efficiency without compromising quality. Meanwhile, the corrugation has become one main concern among all kinds of rail diseases thanks to the increasing vehicle speed. For this reason, one purpose of this paper is to design a new fast rail-grinding device with the open-structured abrasive belt for the corrugation treatment. Although many scholars have studied the problem of dynamic wheel-rail interaction [14–16], there is no public article focusing on the dynamic characteristics of the current rail-grinding car, much less that of the novel grinding car proposed in this paper. Therefore, another purpose of the paper is to analyze the working performance of the designed car.

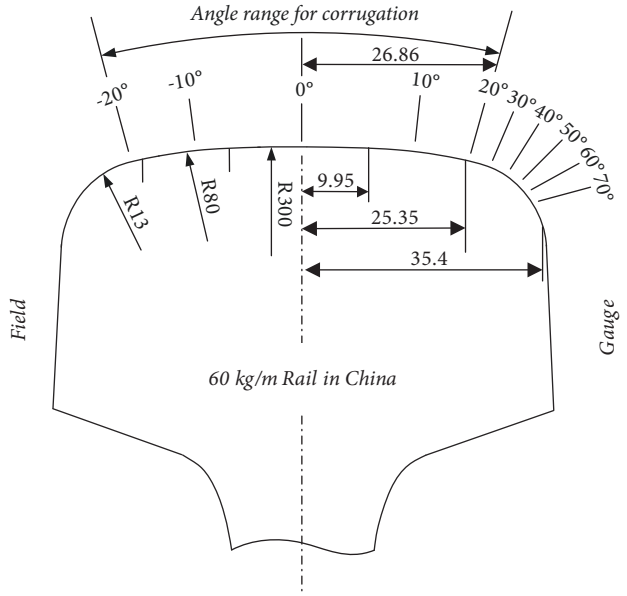

Figure 1: The grinding angle range for the rail corrugation. (unit: mm).

This paper is structured as follows. Section 2 illustrates the designing process and the virtual model of the novel rail-grinding car. In Section 3, the dynamic simulation modeling in SIMPACK software [17–19] is given. Finally, the dynamic performances of the designed car on both the straight line and the curve track are compared and discussed in Section 4.

2. Design and Modeling of Novel Fast Rail-Grinding Car

2.1. Analysis on the Engineering Requirements and Constraints. The rail corrugation describes the phenomenon of the longitudinal irregularity of the rail top. It generally refers to the maximum grinding angle range from -20° to +20° of rail profile, as shown in Figure 1. Although different locomotives at different speeds can make a significant difference, the rail corrugation can be regarded to be with fixed wavelength, such as the roaring one and the rutting one [20].

For China high-speed railways (CHSR), the wavelength of rail corrugation for high-speed running situation is usually between 120 mm and 150 mm. For low speed, it is normally from 60 mm to 80 mm. The average depth of the rail corrugation is less than 0.1 mm. Based on that, referring to traditional planer process, the plate-typed structure is introduced as the pressing component with a length of 300 mm, whose function is to drive the abrasive belt. Furthermore, it can be seen from Figure 1 that the rail profile is composed of several segment arcs with different radii of curvature. Theoretically, the pressing component can be designed to be the integrated pressing plate (see Figure 2(a)) or the one made up of separate pressing plates (see Figure 2(b)). Considering the grinding effect and the cost performance, the integrated pressing plate that matches the rail profile for the grinding angle range from -20° to +20° is finally chosen here.

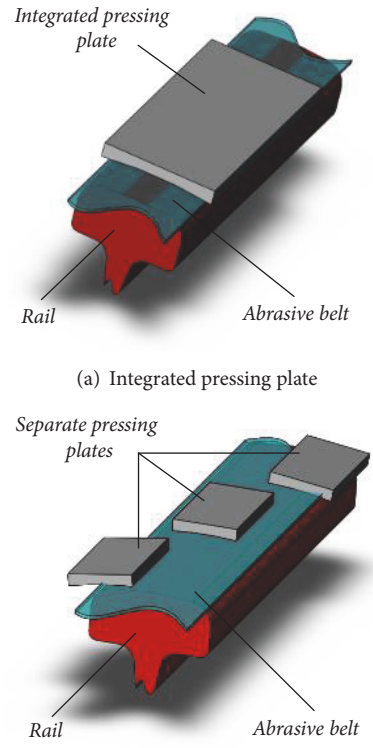

(a) Integrated pressing plate

(b) Separate pressing plates

Figure 2: Different design schemes for the pressing component.

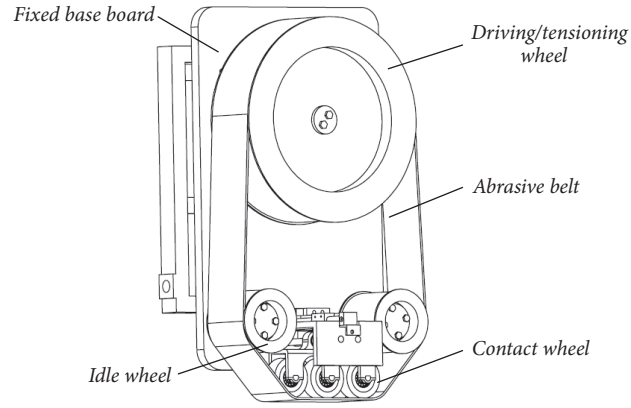

Figure 3: Rail-grinding device using a closed-structured abrasive belt.

According to the actual engineering requirements of CHSR, the ideal working distance of the fast rail grinding train per operation is generally no less than 50-60 km, which approximately equals that between adjacent stations. For this point, as one of coated abrasive tools, the closed-structured abrasive belt with fairly limited abrasives (as shown in Figure 3) hardly satisfies such long working distance. Therefore, the open-structured abrasive belt form is much adopted for the fast rail-grinding equipment, which is also restricted by the document named as *Assembly Technical Conditions of*

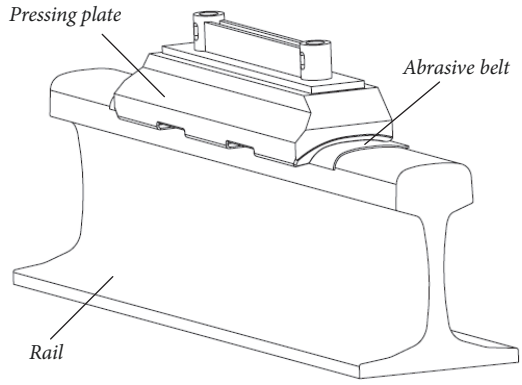

Figure 4: Digital model of the pressing plate.

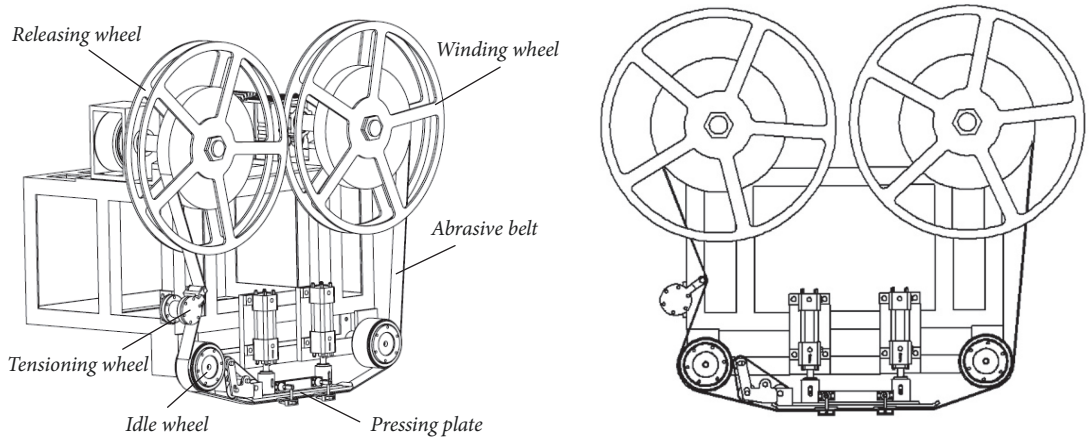

(a) Axonometric drawing (b) Frontal view

Figure 5: The digital model of the wheel system.

Rail Grinding Car formulated by China Railway Corporation [15, 21]. For example, the dimension limitation of the rail-grinding car is strictly given as follows: length ≤3820 mm, width ≤2512 mm, and height ≤1150 mm.

2.2. Design and Digital Modeling of the Rail-Grinding Car. As a complex mechanical system, the rail-grinding car with the open abrasive belt contains many components. The cores belong to the pressing component and the wheel system, which supports and drives abrasive belt. Figure 4 shows the digital model of the designed pressing plate and its relative position to abrasive belt and rail. Its whole length is 300 mm and the width is 52 mm. The working surface can integrally produce the required rail profile with the grinding angle range from -20° to +20°. Meanwhile, the working surface of the pressing plate is also slotted to ensure the chip removal efficiency assisted by high pressure gas.

The wheel system for the open-structured abrasive belt includes the winding wheel, the releasing wheel, the idler, and the tensioning wheel, as shown in Figure 5. The physical dimension of the winding wheel and the releasing wheel is a key factor, which directly determines the length of the abrasive belt and the working distance of the rail-grinding car. The required working distance is 50 km. The average grinding depth is 0.08 mm. The effective grinding width of the abrasive belt is 45 mm. The grinding ratio (the ratio of the removed metal mass to the abrasive belt wear mass) is 300 [22] decided by the experiment using the 36# ceramic abrasive belt. It means the total length of the abrasive belt should be about 160 m. That is to say, the length of the abrasive belt for each grinding unit is 80 m. Considering the thickness of the abrasive belt (1.7 mm) and the minimum diameter (100 mm), the maximum diameter of the winding wheel and the releasing wheel is required to be more than 540 mm.

The final rail-grinding car with the open abrasive belt is shown in Figure 6. Its design parameters are listed in Table 1. Like current facing grinding car by the abrasive wheel, the proposed rail-grinding car here is designed to own two statuses: the hanging state without grinding and the working state with grinding. In the hanging state, the rail-grinding car is lifted to a specific height by four hydraulic cylinders. Only for working state, the rail grinding car is free to propel the abrasive belt to contact the rail top and then do the

Table 1: Main design parameters of the grinding car.

No	Parameters	Values
1	Length×Width×Height of the grinding car (mm)	3140×2500×1050
2	Mass of the grinding car (t)	2.631
3	Number of the grinding units	4
4	Working speed of the grinding car (km/h)	60-80
5	Rotatation speed of the abrasive belt (m/s)	0.05-0.1
6	Average grinding depth (mm)	0.08
7	Length of the abrasive belt of each grinding unit (m)	80
8	Outer diameters of the winding and releasing wheel (mm)	540
9	Length of the pressing plate (mm)	300
10	Effective width of the pressing plate (mm)	45
11	Range of grinding angle (°)	-20 - +20
12	Working distance (km)	≥50

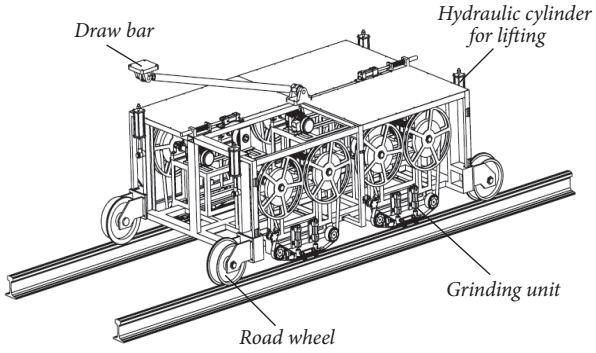

Figure 6: Digital model of the grinding car applying the open-structured abrasive belt.

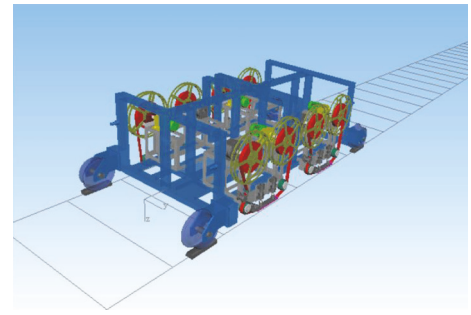

Figure 7: Dynamic simulation model of the fast rail-grinding car using open-structured abrasive belt.

grinding. In addition, the back of abrasive belt that fits the working surface of pressing plate should be termly added with the graphite to raise the wear resistance of pressing plate.

3. Dynamic Modeling of the Fast Rail-Grinding Car

3.1. Dynamic Simulation Modeling in SIMPACK Software. The dynamic simulation model of the rail-grinding car is built in SIMPACK, as shown in Figure 7. The crucial components such as the road wheel, the framework, the wheel system, and the grinding unit are all contained. Each component is defined by the parameters including quality, rotary inertia, center of gravity, stiffness, and damping. Meanwhile, the force elements and the constraints are used to represent the relationship between the components. For instance, the road wheels are connected to the rails through the wheel-rail contact coupling. They are also hinged to the axle by rotating hinge. Similarly, the framework with six degrees of freedom is linked to the axle through the suspension force. Besides, Table 2 lists the main dynamic parameters of the grinding car.

As we know, the rail irregularity excitations in all directions can be transmitted to the crucial components in the form of vibrations and thus have a great influence on the results of the dynamic simulation. To investigate the performance of the fast rail-grinding car more truly, the lateral and vertical excitations from China Wuhan-Guangzhou high-speed railway (see Figure 8) are imported into the dynamic simulation model. Figure 9 shows the frequency spectrums of track excitations of China Wuhan-Guangzhou high-speed railway.

3.2. Assessment Criteria of Dynamic Simulation. The vehicle system dynamics mainly involves the running safety, the stability, and the curve passage capacity. Here, the four dynamic indices including the lateral vibration acceleration, the vertical vibration acceleration, the axle transverse force, and the derailment coefficient are taken into account. According to the China National Standard *Dynamic Performance Evaluation and Test Method for Particular Class Vehicles and Tracked Machine* [23], the maximum allowable values of the lateral and vertical vibration accelerations are, respectively, 4.91 m/s^2 and 6.87 m/s^2. If the number of noncompliance incidents in 100 km railway was no more than three, the assessment would be thought to be qualified. Further, the first limit of the derailment coefficient (the ratio of the lateral force to

Table 2: Main dynamic parameters of the grinding car.

No	Parameters	Values
1	Mass of the grinding car (t)	2.631
2	Moment of inertia of the grinding car $x/y/z$ (t·m^2)	15.3/67/63.5
3	Position of the center of the mass $x/y/z$ (mm)	1395/0/260
4	Mass of each road wheel (kg)	53.2
5	Moment of inertia of the grinding car $x/y/z$ (kg·m^2)	0.37/0.76/0.37
6	Diameter of each road wheel (mm)	350
7	Inclination of the draw bar (°)	25
8	Length of the draw bar (mm)	1800
9	Stiffness of the draw bar (kN/m)	2000
10	Damping of the draw bar (kN·s/m)	3
11	Tangential resistance of each pressing plate (kN)	1.2
12	DOF of the joints at each road wheel	γ
13	DOF of the joints at each side of the draw bar	γ, ψ
14	DOF of the pressing plate	z
15	DOF of the grinding car	$x, y, z, \varphi, \gamma, \psi$

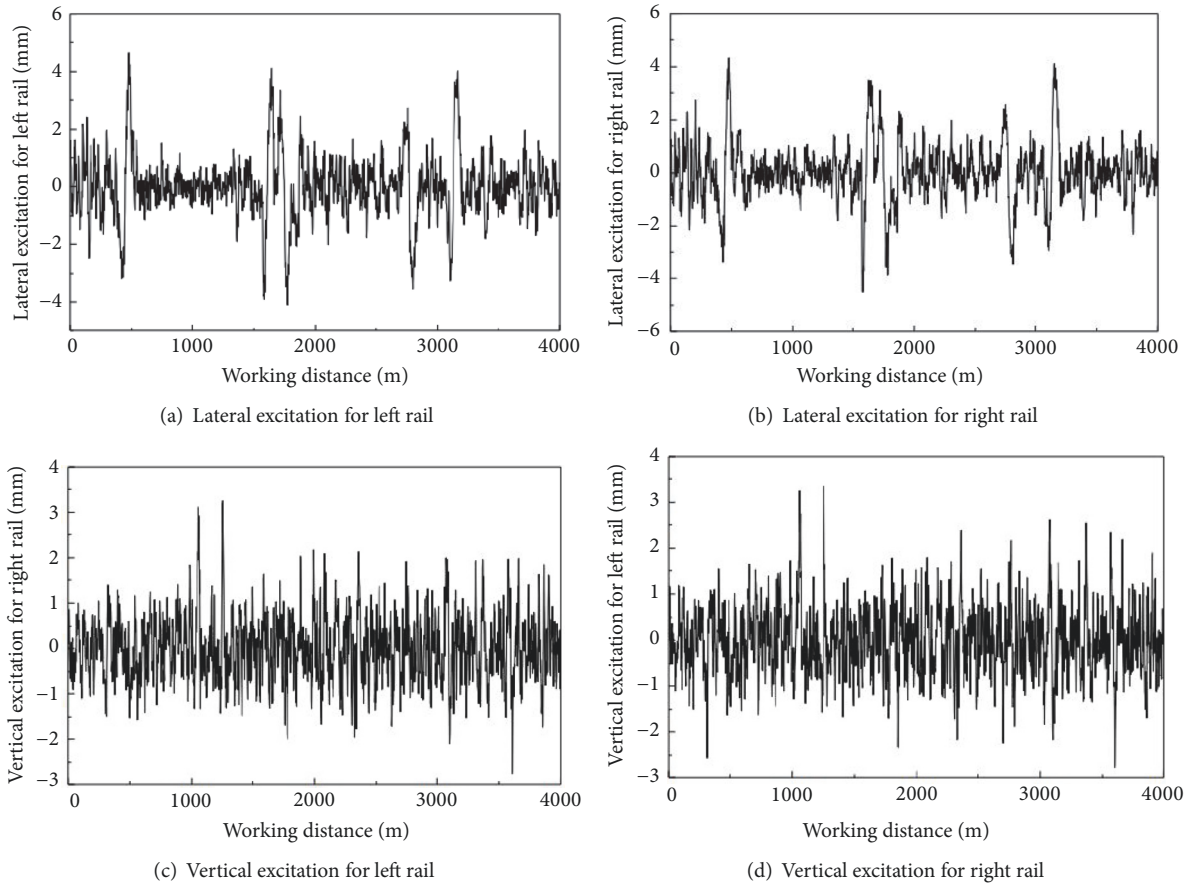

(a) Lateral excitation for left rail

(b) Lateral excitation for right rail

(c) Vertical excitation for left rail

(d) Vertical excitation for right rail

Figure 8: Lateral and vertical excitations of China Wuhan-Guangzhou high-speed railway.

the vertical force acting on the wheel) is less than 1.2 and the second limit of the derailment coefficient (safety margin criteria) is no more than 1.0. Besides, through the wheel static load, the maximum axle transverse force can be calculated as 35.22 kN.

4. Analysis and Discussion of Dynamic Simulation Results

4.1. Straight Line Grinding Condition. Among the four dynamic indices, the derailment coefficient should be paid

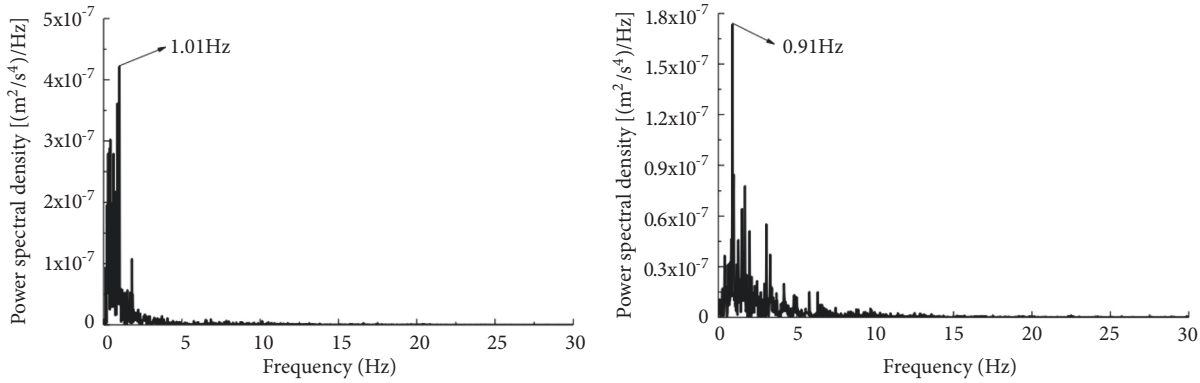

(a) Lateral PSD (b) Vertical PSD

Figure 9: Frequency spectrums of track excitations of China Wuhan-Guangzhou high-speed railway.

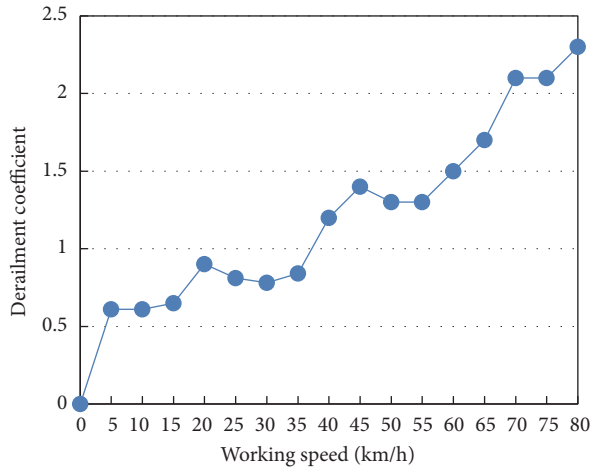

Figure 10: Derailment coefficient without damping.

extraordinary attention due to the high working speed of the rail-grinding car. Figure 10 shows the simulation results in the absence of damping for the working speed from 0 to 80 km/h. It is clear that the derailment coefficient has already been as high as the first limit (1.2), only when the working speed is 42 km/h. As for the design working speed, 60 to 80 km/h, this index is undisputed and unqualified. The main reason is that the mechanical joint between the rail-grinding car and the vehicle is frail, because the rail-grinding car is generally suspended underneath the vehicle through the draw bar. So, the certain damping needs to be imposed on the mechanical joint to restrict the freedom of the rail-grinding car, which is very different from that of the rail-grinding car with the closed abrasive belt or the abrasive wheel that usually has the fairly low working speed: 7 to 15 km/h. The damping was applied vertically at the four corners above the grinding car's frame (the position of the lifting cylinders), which connected the vehicle and the grinding car. The value of the damping coefficient is 7.8 kN·s/m for each.

Afterward, in the premise of damping, the dynamic simulations of the four dynamic indices, the lateral vibration acceleration, the vertical vibration acceleration, the axle transverse force, and the derailment coefficient, are performed and the results are shown in Figure 11. It can be seen that the four dynamic indices display a growth trend as a whole with the increase of the working speed. The maximum lateral vibration acceleration (2.50 m/s^2), the maximum vertical vibration acceleration (5.8 m/s^2), the maximum axle transverse force (2.1 kN), and the maximum derailment coefficient (0.59) are strictly within their limits.

4.2. Curve Grinding Condition. By choosing the options "STR, BLO, CIR, BLO, STR" in SIMPACK software, the curve railway "Line-Easement curve-Circular curve-Easement curve-Line" is added into the dynamic simulation model. Figure 12 shows the dynamic simulation results for the curve line condition. As seen in Figures 12(a) and 12(b), both the lateral vibration acceleration and the vertical vibration acceleration show a growth trend with the increasing radius of curvature. The higher working speed produces the bigger values of the lateral vibration acceleration and the vertical vibration acceleration. The maximum lateral

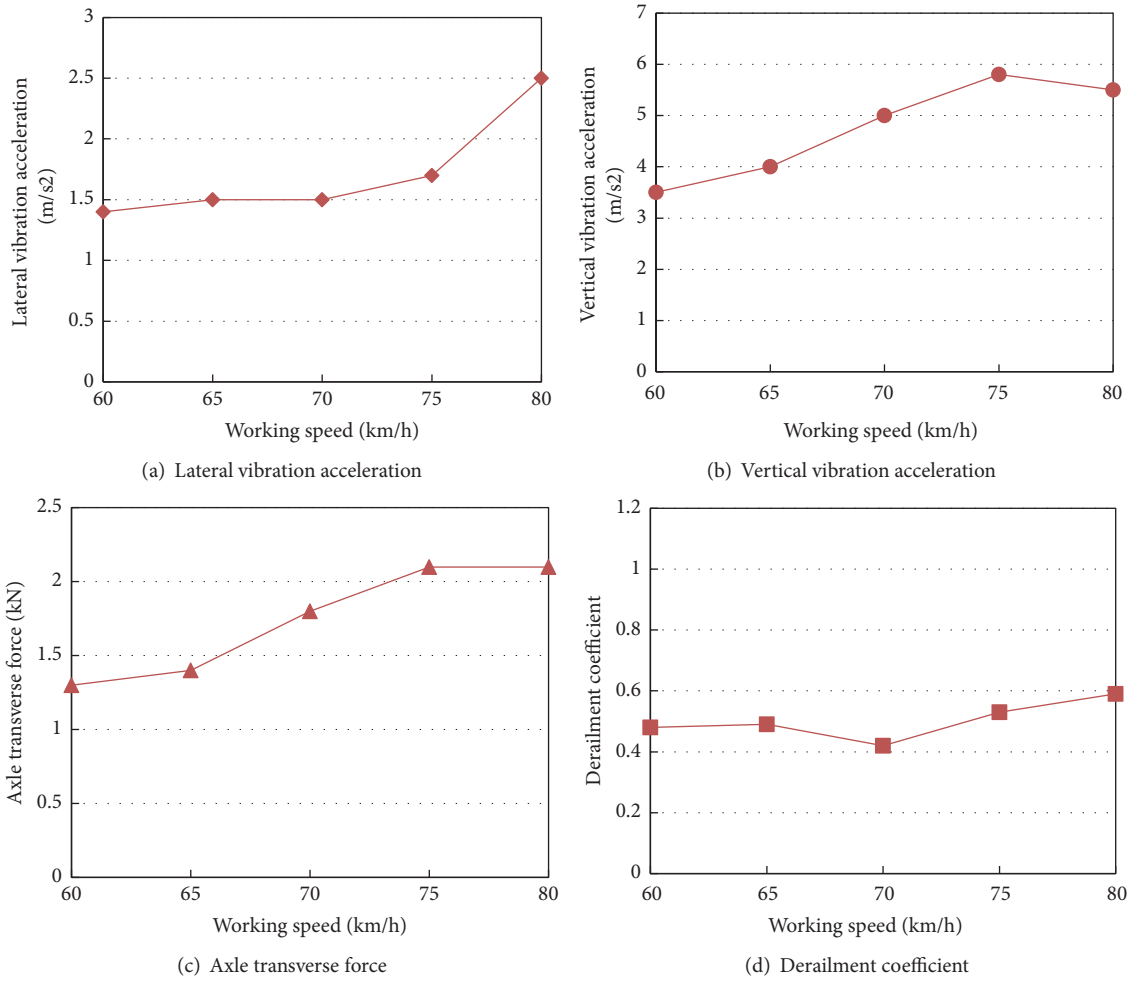

Figure 11: Dynamic simulation results for the straight line condition.

vibration acceleration (2.51 m/s^2) and the maximum vertical vibration acceleration (5.43 m/s^2) meet the requirement. On the contrary, the axle transverse force and the derailment coefficient decline with the increase of the radius of curvature, as shown in Figures 12(c) and 12(d). And the maximum axle transverse force (3.1 kN) and the maximum derailment coefficient (0.67) are also within the demanding range and thus thought to be qualified.

Comparing the results of curve line and the straight line, some irregularities can be found there. For example, by considering Figure 12(d) with speed of 80 km/h and radius of curvature equal to 1000 mm, the decreasing derailment coefficient is lesser than the limit of 0.59, as it is reported on in Figure 11(d). The reason for that can be explained as follows. The values of the analyzed parameters in Figure 12 are average values calculated by a series of fluctuating data, which are output by the SIMPACK. It is known that the SIMPACK simulation is a kind of stochastic processes, so all the observed parameters keep changing along the simulation time. In order to have an overview of the change tendency of those evaluation parameters affected by the radius of curvature, the mean of the relatively stable peak segment data was extracted as the result for the comparative analysis. Therefore, it exists some irregularity as mentioned by the reviewer. Besides, the irregularity questioned by the reviewer may be also caused by the artificial error when deciding the effective data segment.

5. Conclusions

A new fast rail-grinding car with the open-structured abrasive belt was designed for the corrugation treatment of high-speed railways. It includes four individual grinding units composed of the pressing component and the wheel system and is supposed to eliminate the corrugation referring to the grinding angle range from -20° to +20° for the rail profile under the working speed from 60 km/h to 80 km/h.

The dynamic simulations were implemented based on the SIMPACK. The results show that the derailment coefficient is unqualified since working speed over 42 km/h. Therefore, the certain damping was imposed on the mechanical joint to restrict the freedom of the rail-grinding car. Furthermore, to ensure the authenticity of the simulation environment, the lateral and vertical excitations from

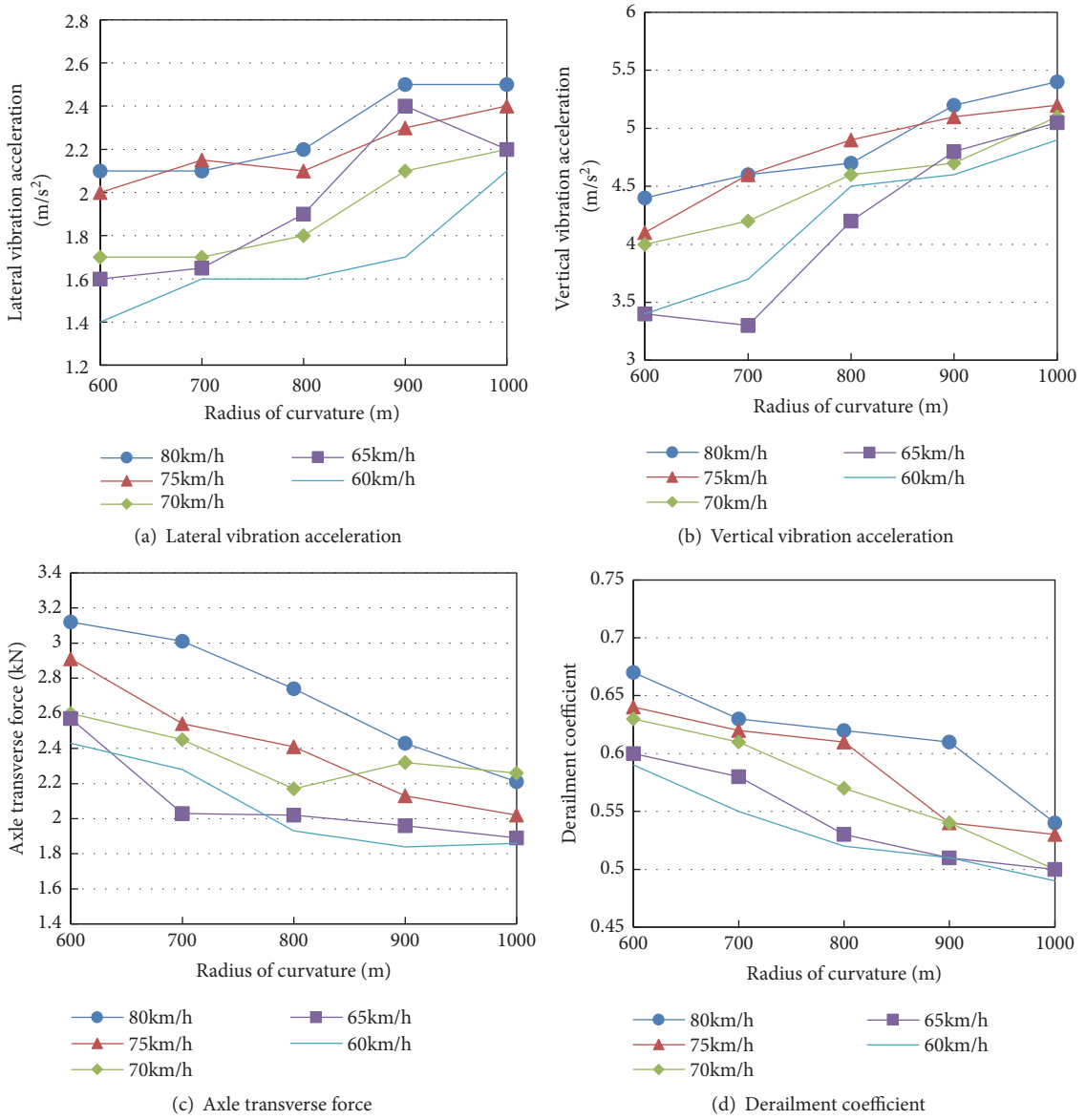

Figure 12: Dynamic simulation results for the curve line condition.

China Wuhan-Guangzhou high-speed railway are imported. The four dynamic indices were investigated. Results basically satisfy the limits of the indices, which has verified the design rationality of the new fast rail-grinding car.

Data Availability

The data used in this manuscript to support the findings of this study are available from the corresponding author (Mr. Wenxi Wang 14116345@bjtu.edu.cn) upon request.

Conflicts of Interest

The authors declare that they have no conflicts of interest.

Acknowledgments

The authors would like to thank the financial support from the Fundamental Research Funds for the Central Universities (Grant no. 2019JBM050) and the help of paper writing from Prof. Jianyong Li and Dr. Vipul Vijigiri.

References

[1] D. F. Cannon, K.-O. Edel, S. L. Grassie, and K. Sawley, "Rail defects: an overview," *Fatigue & Fracture of Engineering Materials & Structures*, vol. 26, no. 10, pp. 865–886, 2003.

[2] M. Steenbergen, "Rolling contact fatigue in relation to rail grinding," *Wear*, vol. 356-357, pp. 110–121, 2016.

[3] S. Zhi, J. Li, and A. M. Zarembski, "Grinding motor energy saving method based on material removal model in rail grinding

processes," *International Journal of Precision Engineering and Manufacturing - Green Technology*, vol. 2, no. 1, pp. 21–30, 2015.

[4] J. I. Real, C. Zamorano, J. L. Velarte, and A. E. Blanco, "Development of a vehicle–track interaction model to predict the vibratory benefits of rail grinding in the time domain," *Journal of Modern Transportation*, vol. 23, no. 3, pp. 189–201, 2015.

[5] A. M. Zarembski, "Grinding as part of rail management strategy," *Railway Track and Structure*, vol. 104, no. 6, pp. 55–58, 2008.

[6] Y. M. Liu, T. Y. Yang, Z. He, and J. Y. Li, "Analytical modeling of grinding process in rail profile correction considering grinding pattern," *Archives of Civil and Mechanical Engineering*, vol. 18, no. 2, pp. 669–678, 2018.

[7] P. A. Cuervo, J. F. Santa, and A. Toro, "Correlations between wear mechanisms and rail grinding operations in a commercial railroad," *Tribology International*, vol. 82, pp. 265–273, 2015.

[8] J. F. Santa, A. Toro, and R. Lewis, "Correlations between rail wear rates and operating conditions in a commercial railroad," *Tribology International*, vol. 95, pp. 5–12, 2016.

[9] R. Singleton, M. B. Marshall, R. Lewis, and G. Evans, "Rail grinding for the 21st century - taking a lead from the aerospace industry," *Proceedings of the Institution of Mechanical Engineers, Part F: Journal of Rail and Rapid Transit*, vol. 229, no. 5, pp. 457–465, 2015.

[10] E. Uhlmann, P. Lypovka, L. Hochschild, and N. Schröer, "Influence of rail grinding process parameters on rail surface roughness and surface layer hardness," *Wear*, vol. 366-367, pp. 287–293, 2016.

[11] Linsinger, http://www.linsinger.com/portfolio/sf03-ffs/?lang=en.

[12] W. Fan, Y. Liu, X. Song, J. Cheng, and J. Li, "Influencing mechanism of rubber wheel on contact pressure and metal removal in corrugated rail grinding by abrasive belt," *Journal of Manufacturing Science and Engineering*, vol. 140, no. 12, pp. 12450-12451, 2018.

[13] Z. He, J. Y. Li, Y. M. Liu, M. Nie, and W. G. Fan, "Investigating the effects of contact pressure on rail material abrasive belt grinding performance," *The International Journal of Advanced Manufacturing Technology*, vol. 93, no. 1-4, pp. 779–786, 2017.

[14] A. A. Shabana, M. Tobaa, H. Sugiyama, and K. E. Zaazaa, "On the computer formulations of the wheel/rail contact problem," *Nonlinear Dynamics*, vol. 40, no. 2, pp. 169–193, 2005.

[15] S. Kulkarni, C. M. Pappalardo, and A. A. Shabana, "Pantograph/catenary contact formulations," *Journal of Vibration and Acoustics*, vol. 139, no. 1, p. 011010, 2017.

[16] E. E. Magel and J. Kalousek, "The application of contact mechanics to rail profile design and rail grinding," *Wear*, vol. 253, no. 1-2, pp. 308–316, 2002.

[17] M. Ignesti, A. Innocenti, L. Marini, E. Meli, and A. Rindi, "Development of a model for the simultaneous analysis of wheel and rail wear in railway systems," *Multibody System Dynamics*, vol. 31, no. 2, pp. 191–240, 2014.

[18] J. Xu, P. Wang, L. Wang, and R. Chen, "Effects of profile wear on wheel-rail contact conditions and dynamic interaction of vehicle and turnout," *Advances in Mechanical Engineering*, vol. 8, no. 1, pp. 1–14, 2016.

[19] M. Ignesti, M. Malvezzi, L. Marini, E. Meli, and A. Rindi, "Development of a wear model for the prediction of wheel and rail profile evolution in railway systems," *Wear*, vol. 284-285, pp. 1–17, 2012.

[20] S. L. Grassie, "Rail corrugation: characteristics, causes, and treatments," *Proceedings of the Institution of Mechanical Engineers, Part F: Journal of Rail and Rapid Transit*, vol. 223, no. 6, pp. 1–16, 2009.

[21] "Assembly technical conditions of rail grinding device, China Railway Industry Standard, TJ/GW131-2015," Tech. Rep., China Railway Corporation, 2015 (Chinese).

[22] Y. Liu, Z. He, R. Wang, and J. Li, "Experimental investigation on grinding behavior of abrasive belt for rail specimen," *Journal of Basic Science and Engineering*, vol. 25, no. 2, pp. 419–426, 2017 (Chinese).

[23] "Dynamic performance evaluation and test method for particular class vehicles and tracked machine, China National Standard, GB/T 17426-1998," Tech. Rep., National Quality Technical Supervise Department, 1998 (Chinese).